

# Synthesis and Characterization of Octahedral Molecular Sieves (OMS-2) Having the Hollandite Structure

Roberto N. DeGuzman,<sup>†</sup> Yan-Fei Shen,<sup>†</sup> Edward J. Neth,<sup>†</sup> Steven L. Suib,<sup>\*,†,‡</sup>  
Chi-Lin O'Young,<sup>\*,§</sup> Steven Levine,<sup>⊥</sup> and John M. Newsam<sup>⊥</sup>

Charles E. Waring Laboratory, Department of Chemistry, U-60, University of Connecticut, Storrs, Connecticut 06269-3060; Institute of Materials Science and Department of Chemical Engineering, University of Connecticut, Storrs, Connecticut 06269; Texaco Research Center, Texaco, Inc., P.O. Box 509, Beacon, New York 12508; and Biosym Technologies, Inc., 9685 Scranton Road, San Diego, California 92121

Received February 17, 1994. Revised Manuscript Received March 21, 1994\*

Hollandite and cryptomelane materials have been prepared using two different methods. Octahedral molecular sieve (OMS) having the  $2 \times 2$  hollandite structure with a one-dimensional pore diameter of 4.6 Å. Synthetic cryptomelane or OMS-2 can be formed by refluxing or autoclaving an acidic solution of  $\text{KMnO}_4$  and  $\text{Mn}^{2+}$ . Temperature, pH, and counteraction are important synthetic parameters. The hollandite formed shows thermal stability up to 600 °C. OMS-2 formed by oxidation of  $\text{Mn}^{2+}$  under basic conditions and calcined at higher temperature (200–800 °C) is thermally stable up to 800 °C. X-ray powder diffraction and electron diffraction patterns have been simulated that show good agreement with experimental data supporting a tetragonal crystal system in the  $I4/m$  space group. Hollandites were also prepared in the presence of other transition-metal ions such as  $\text{Cu}^{2+}$  and  $\text{Fe}^{3+}$ . The  $\text{Cu}^{2+}$ - and  $\text{Fe}^{3+}$ -doped OMS-2 materials were prepared by refluxing a solution of  $\text{MnO}_4^-$  and  $\text{Mn}^{2+}$  with  $\text{Cu}^{2+}$  or  $\text{Fe}^{3+}$ . Electron paramagnetic resonance (EPR) data show that OMS-2 materials synthesized in the presence of  $\text{Cu}^{2+}$  and  $\text{Fe}^{3+}$  contain nonexchangeable  $\text{Mn}^{2+}$ . EPR data for Cu-OMS-2 showed a characteristic six-line pattern with a  $g$  value of 2.0 and an  $A$  value of 85 G indicative of octahedral  $\text{Mn}^{2+}$  coordination. The  $\text{Mn}^{2+}$  EPR peaks in Fe-OMS-2 showed similar  $g$  and  $A$  values. EPR spectra, ion-exchange data, X-ray diffraction patterns, and theoretical simulations of diffraction data suggest that  $\text{Cu}^{2+}$  and  $\text{Fe}^{3+}$  are located in the tunnels of OMS-2.

## Introduction

We have recently reported the synthesis, characterization, and potential applications of several octahedral molecular sieve (OMS) materials<sup>1-4</sup> consisting of  $\text{MnO}_6$  octahedra which are linked at vertices and edges. One particular material, synthetic todorokite has been designated OMS-1 which has a 3 by 3 tunnel structure having a pore size of about 6.9 Å.<sup>1,2</sup> The composition of OMS-1 is  $\text{Mg}^{2+}_{0.98-1.35}\text{Mn}^{2+}_{1.89-1.94}\text{Mn}^{4+}_{4.38-4.54}\text{O}_{12}\cdot 4.47-4.55\text{H}_2\text{O}$ , and it is believed to be a mixed-valent species having primarily  $\text{Mn}^{4+}$  but also some  $\text{Mn}^{3+}$  and  $\text{Mn}^{2+}$  based on an average oxidation state of about 3.6 and on various spectroscopic data such as X-ray photoelectron spectroscopy and electron paramagnetic resonance (EPR).<sup>1-3</sup> The structure of OMS-1 is given in Figure 1.

A related structure is the  $2 \times 2$  structure of the mineral hollandite which is also shown in Figure 1. The  $\text{K}^+$  form of hollandite is known as cryptomelane, and it has a

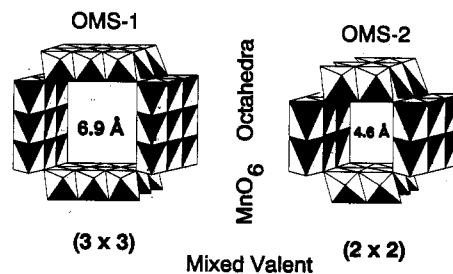


**Figure 1.** Tunnel structures of octahedral molecular sieve (OMS) manganese oxides. OMS-1 is synthetic todorokite with a  $3 \times 3$  structure. The basic structure of OMS-2 consists of two sheets of  $\text{MnO}_6$  octahedra joined at edges to form the  $2 \times 2$  hollandite tunnel structure. Tunnel counteraction is  $\text{Ba}^{2+}$  for hollandite,  $\text{K}^+$  for cryptomelane (depicted), and  $\text{Pb}^{2+}$  for coronadite.

composition of  $\text{KMn}_5\text{O}_{16}$ .<sup>3</sup> The pore size of the tunnel is about 4.6 Å. This material has been designated OMS-2, which is a synthetic cryptomelane that is also mixed valent and has an average oxidation state of 3.9.<sup>1,2</sup> The literature suggests<sup>5-18</sup> that only a small amount of  $\text{Mn}^{3+}$  exists in cryptomelane and that the majority of manganese is  $\text{Mn}^{4+}$ .

<sup>†</sup> Department of Chemistry, University of Connecticut.  
<sup>‡</sup> Department of Materials Science and Chemical Engineering, University of Connecticut.  
<sup>§</sup> Texaco Research Center.  
<sup>⊥</sup> Biosym Technologies, Inc.  
\* To whom correspondence should be addressed.  
\* Abstract published in *Advance ACS Abstracts*, May 1, 1994.  
(1) Shen, Y. F.; Zenger, R. P.; DeGuzman, R. N.; Suib, S. L.; McCurdy, L.; Potter, D.; O'Young, C. L. *J. Chem. Soc., Chem. Commun.* 1992, 1213-1214.  
(2) Shen, Y. F.; Zenger, R. P.; DeGuzman, R. N.; Suib, S. L.; McCurdy, L.; Potter, D.; O'Young, C. L. *Science* 1993, 260, 511-515.  
(3) DeGuzman, R. N.; Shen, Y. F.; Suib, S. L.; Shaw, B. R.; O'Young, C. L. *Chem. Mater.* 1993, 5, 1395-1400.  
(4) Suib, S. L.; Iton, L. E. *Chem. Mater.*, in press.

(5) Post, J. E.; Von Dreele, R. B.; Buseck, P. R. *Acta Crystallogr.* 1982, B38, 1056.  
(6) Giovanilli, R.; Balmer, B. *Chimia* 1981, 35, 53.  
(7) Chen, C. C.; Golden, D. C.; Dixon, J. B. *Clays Clay Miner.* 1986, 34, 565.  
(8) Post, J. E.; Bish, D. L. *Am. Miner.* 1989, 74, 913.  
(9) Clearfield, A. *Chem. Rev.* 1988, 88, 125.  
(10) Potter, R. M.; Rossman, G. R. *Am. Miner.* 1979, 64, 1199.  
(11) Turner, S.; Buseck, P. R. *Science* 1981, 212, 1024.  
(12) Wadsley, A. D. *Am. Miner.* 1950, 35, 485.  
(13) Wong, S. T.; Cheng, S. *Inorg. Chem.* 1992, 31, 1165.

OMS-2 has been prepared by reflux and hydrothermal alteration methods,<sup>3,4</sup> and the resultant materials have broad X-ray diffraction lines and concomitant small particle sizes (on the order of 250 Å) as compared to hollandites that have been prepared with flux or solid-state methods.<sup>18</sup>

We are particularly interested in OMS materials because they are cation-exchange materials<sup>1,2</sup> and are microporous<sup>1,2</sup> as are zeolites. OMS-1 and OMS-2 are both small particle size materials having large surface areas up to 250 m<sup>2</sup>/g which result in outstanding catalytic materials for oxidation reactions.<sup>1,2</sup> The acidities of OMS-1 and OMS-2 can be varied by altering the method of preparation, by specific activation, and by doping these materials with transition-metal cations either before or after crystallization.<sup>2</sup>

Hollandite,<sup>5-6</sup> cryptomelane,<sup>7</sup> and coronadite<sup>8</sup> are structurally related manganese oxide materials that have different cation contents such as Ba<sup>2+</sup>, K<sup>+</sup>, and Pb<sup>2+</sup>, respectively.<sup>9,10</sup> They have similar structures based on double chains of edge-sharing MnO<sub>6</sub> octahedra; see Figure 1. These sheets of MnO<sub>6</sub> form channels that contain water and ions such as K<sup>+</sup>, Ba<sup>2+</sup>, and Pb<sup>2+</sup> in cryptomelane, hollandite, and coronadite, respectively. These manganese oxide minerals have the 2 × 2 structure as shown in Figure 1, the tunnel pore size bordered by two MnO<sub>6</sub> octahedra on both sides. Other manganese oxide minerals with tunnel structures are todorokite<sup>1,2,11</sup> (3 × 3), psilomelane<sup>12</sup> (3 × 2), and romanecchite (3 × 2).

Buserite and birnessite<sup>13</sup> are structurally related tetravalent manganese oxide minerals with a layer structure containing cations and water between the layers. Birnessite is the partially dehydrated form of buserite; the interlayer distance is about 7.0 Å.<sup>14</sup> Each layer consists of MnO<sub>6</sub> octahedra forming sheets by edge sharing. The Na<sup>+</sup> ion can be quantitatively ion-exchanged by other cations like K<sup>+</sup>, Ba<sup>2+</sup>, and Pb<sup>2+</sup>. In addition, birnessite can be prepared by oxidation of Mn<sup>2+</sup> in basic solution or by reduction of KMnO<sub>4</sub> by HCl. One route to the preparation of hollandite is by ion exchange of Na-buserite with K<sup>+</sup>, Ba<sup>2+</sup>, or Pb<sup>2+</sup> with subsequent partial dehydration of the exchanged buserites to form birnessites. Subsequent heat treatment of the exchanged birnessites at 200–800 °C will produce hollandites.<sup>15</sup>

Another route for the preparation of hollandite is by heating amorphous MnO<sub>2</sub> formed by the reduction of Mn<sup>2+</sup> by KMnO<sub>4</sub> in acidic media. The MnO<sub>2</sub> can be heated from 60 to 80 °C,<sup>16</sup> boiled, or treated hydrothermally. An important factor in this synthesis is the presence of K<sup>+</sup> during heat treatment.

In this paper we describe the synthesis and characterization of OMS-2 materials. A major emphasis has been to determine ranges of composition, the different oxidation states of manganese, and the extent to which doping with various transition metals can occur, in particular divalent cations. By inserting divalent cations into OMS it may be possible to alter electronic, catalytic, and structural properties. The choice of Cu<sup>2+</sup>, Fe<sup>2+</sup>, and other divalent cations is dictated by sizes, charges, and polarizabilities<sup>1-4</sup>

that are similar to Mn<sup>2+</sup> for which these cations may substitute. Cu<sup>2+</sup> is readily observed with electron paramagnetic resonance (EPR). Since 2 × 2 materials can have variable composition and can be prepared by a variety of methods,<sup>1-18</sup> the resultant degree of mixed valency and structure can vary. We have therefore, undertaken Rietveld refinement studies to study the structure of OMS-2. Thermal stability and morphological properties are also reported.

## Experimental Section

**Synthesis of Hollandite.** Hollandite was prepared by two general methods, referred to as methods 1 and 2. Method 1 involved refluxing a solution of KMnO<sub>4</sub> and Mn<sup>2+</sup>. A typical synthesis was as follows: 5.89 g of KMnO<sub>4</sub> in 100 mL of water was added to a solution of 8.8 g of MnSO<sub>4</sub>·H<sub>2</sub>O in 30 mL of water and 3 mL concentrated HNO<sub>3</sub>. The solution was refluxed at 100 °C for 24 h, and the product was filtered, washed, and dried at 120 °C. A variation of this method involved pouring a solution of KMnO<sub>4</sub> and Mn<sup>2+</sup> into a Teflon-lined Parr autoclave (125-mL capacity) and heated in an oven at 100 °C for 24 h. Capped glass bottles (200 mL) were also used for such syntheses.

Method 2 involved a variation of a procedure used by Giovanili and Balmer<sup>9</sup> for the preparation of hollandite. Their method involved formation of a layered phylomanganate (buserite) followed by ion-exchange with K<sup>+</sup>, partial dehydration to K-birnessite, and calcination at high temperature. The ion-exchange step was skipped in our preparation because KOH was used instead of NaOH. A typical preparation is as follows: a solution of 35 g of KOH in cold 200 mL of water was added to a solution of 30 g of MnSO<sub>4</sub>·H<sub>2</sub>O in 200 mL of water. Oxygen gas was bubbled vigorously (about 12 L/min) through the solution for 4 h. The black K-buserite product was washed with water and placed in a furnace at 600 °C for 18–24 h. The yield was about 17.0 g.

**Synthesis of Cu-OMS-2 and Fe-OMS-2.** A modification of method 1 described above was used in the preparation of Cu<sup>2+</sup>- and Fe<sup>3+</sup>-substituted OMS-2 materials. A typical preparation is as follows: 5.89 g of KMnO<sub>4</sub> in 100 mL of water was added to a solution of 8.8 g of MnSO<sub>4</sub>·H<sub>2</sub>O in 30 mL of water and 3 mL of concentrated HNO<sub>3</sub>. Solutions of CuSO<sub>4</sub> or Fe(NO<sub>3</sub>)<sub>3</sub> were added to make a total concentration of Cu<sup>2+</sup> or Fe<sup>3+</sup> of 0.01, 0.1, and 0.37 M. The solutions were refluxed for 24 h, filtered, washed, and dried at 120 °C overnight.

**Characterization Methods.** Powder X-ray diffraction data were collected using a Scintag 2000 PDS with Cu Kα X-ray radiation. A 0.02 step in 2θ/count, 45-kV beam voltage, and 40-mA beam current were used. Thermogravimetric analysis (TGA) was done on a Perkin-Elmer TGA-7 System under oxygen and nitrogen atmospheres. An AMRAY Model 1810 D scanning electron microscope equipped with an AMRAY PV 9800 energy-dispersive X-ray analyzer was used for SEM-EDX experiments. Electron paramagnetic resonance (EPR) spectra were recorded using a Varian E-3 EPR spectrometer equipped with a liquid nitrogen cooling attachment. Hollandite samples (about 0.2 g) were evacuated at 10<sup>-3</sup> Torr and sealed in quartz tubing (o.d. 4.0 mm). Chemical analysis of the cation composition of hollandites was done using atomic absorption spectroscopy (AAS). Hollandite samples were dissolved in dilute HNO<sub>3</sub>-H<sub>2</sub>O<sub>2</sub> solution for AAS experiments and for determination of average oxidation states. The average oxidation number of manganese was determined using the procedure used by Murray et al.<sup>19</sup>

Transmission electron microscopy data were collected on a Phillips EM 420 instrument. Samples were prepared by taking hollandite powders dispersed in acetone and depositing the slurry on a copper grid.<sup>1,2</sup>

**Theoretical Calculations.** The simulated X-ray and electron diffraction patterns for the K-Mn hollandite structures were calculated using modeling software supplied by BIOSYM

(14) Golden, D. C.; Dixon, J. B.; Chen, C. C. *Clays Clay Miner.* 1986, 34, 511.

(15) Ooi, K.; Miyai, Y.; Katoh, S. *Sep. Sci. Technol.* 1987, 22, 1779.

(16) Tsuji, M.; Abe, M. *Solvent Extract. Ion Exch.* 1984, 2, 253.

(17) Vicat, J.; Fanchon, E.; Strobel, P.; Qui, D. T. *Acta Crystallogr.* 1982, B42, 162–167.

(18) Post, J. E.; von Dreele, R. B.; Buseck, P. R. *Acta Crystallogr.* 1982, B38, 1056–1065.

(19) Murray, J. W.; Balistieri, L. S.; Paul, B. *Geochim. Cosmochim. Acta* 1984, 48, 1237.

Technologies of San Diego, CA, including the program InsightII 2.20b and the Diffraction pulldown of the Catalysis 2.0b release.

Lattice parameters for the electron and X-ray powder diffraction simulation on  $K^+$ -substituted Mn-hollandite were taken as follows:  $a = 9.8$ ,  $b = 9.8$ ,  $c = 2.86$ .<sup>25</sup> All angles ( $\alpha$ ,  $\beta$ ,  $\gamma$ ) were taken as  $90^\circ$ ; the unit cell is tetragonal, with space group  $I4/m$ . The X-ray powder calculation was performed between  $5$  and  $60^\circ$   $2\theta$  and the electron diffraction pattern was calculated between  $10$  and  $50^\circ$   $2\theta$  using the 100 zone.

An initial model for the hollandite materials reported here was developed from published data for the mineral cryptomelane<sup>18</sup> and priderite,<sup>28</sup> using lattice parameters determined in this laboratory from electron diffraction studies. On the basis of calculations from electron paramagnetic resonance and X-ray photoelectron spectroscopy studies, the structure was modeled to contain  $Mn^{4+}$  (fraction 0.8) and  $Mn^{3+}$  (fraction 0.2). Refinements employing the Rietveld refinement method were implemented using the program GSAS (General Structure Analysis System) by Larson and von Dreele, Los Alamos National Laboratory, NM. Graphical display and guidance during the process were done using the InsightII 2.2.0/Catalysis 3.0 molecular modeling interface to the GSAS utilities (InsightII, BIOSYM Technologies, San Diego, CA) on a Silicon Graphics XS-24 Iris Indigo workstation. The ORTEP program provided as part of GSAS was used to produce the final plot of the atomic positions.

Rietveld refinement techniques were performed on data collected on a Scintag XDS-2000 X-ray diffraction system. The peaks in the pattern were indexed as a guide for the refinement process. The space group used for the refinement was tetragonal;  $I4/m$ . The area from  $20$ – $60^\circ$   $2\theta$  was refined stepwise, beginning with the scale factor and background coefficients; previously refined parameters were allowed to vary throughout the remainder of the process. The occupancies of  $Mn^{4+}$  and  $Mn^{3+}$  were constrained to give the above ratio (in sum, 1.0) and held that way during the refinement. Background subtraction was performed using a spline curve fit, using eight points along the pattern. A pseudo-Voigt function with  $\gamma = 0.2$  was used to fit the peak profiles. Parameters refined included the background coefficients, scale factors, peak profile coefficients (3), lattice parameters, atomic positions, occupancies, and isotropic temperature factors.

## Results

**Synthesis.** The synthesis of cryptomelane from  $KMnO_4$  and  $Mn^{2+}$  depends on three factors,<sup>20</sup> pH, temperature, and the type of counteraction. When  $KMnO_4$  is added to  $Mn^{2+}$ , amorphous  $MnO_2$  forms. After several hours of heating, even at temperatures as low as  $80^\circ C$ , X-ray diffraction data (vide infra) show the formation of cryptomelane. In this study, solutions of  $KMnO_4$  and  $Mn^{2+}$  were heated by refluxing and by autoclaving to study differences in the cryptomelane products that were formed. The pH of these solutions is an important parameter; heating of these solutions above pH 2.0 produces amorphous  $MnO_2$ . Hollandite forms when the pH is 1.7 or lower. When solutions are autoclaved at temperatures higher than  $120^\circ C$ , pyrolusite forms.

**X-ray Diffraction.** The X-ray powder pattern of cryptomelane formed by refluxing at  $100^\circ C$  for 24 h is

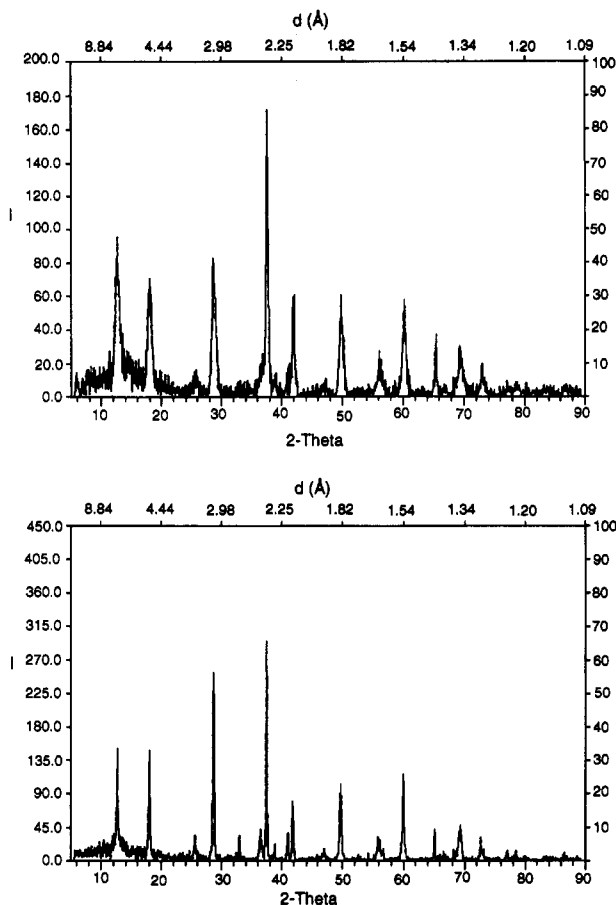


**Figure 2.** X-ray powder diffraction data for hollandite prepared by (a) method 1, refluxing, and (b) method 2, calcination at  $600^\circ C$ .

shown in Figure 2a. The X-ray powder patterns of the cryptomelanes formed by autoclaving, either using Teflon-lined autoclaves or when ordinary capped bottles were used at temperatures of  $100$ – $110^\circ C$  were identical to that presented in Figure 2a. Increasing the time of refluxing, from 24 h to 1 week did not change the X-ray powder pattern; the structure remains essentially that of cryptomelane. No significant differences between the OMS-2 prepared by refluxing or by autoclaving procedures were found with regard to structure by X-ray powder diffraction. Figure 2b shows an X-ray powder pattern of the cryptomelane product formed when method 2 (adapted from Giovanili and Balmer)<sup>6</sup> was used. All the major peaks for cryptomelane are present, but there are some differences in the relative peak heights of the calcined cryptomelane with respect to cryptomelane formed by refluxing (OMS-2). The X-ray powder diffraction data for Cu-OMS-2 and Fe-OMS-2 show that these products also have the cryptomelane structure. The X-ray powder patterns are very similar to those presented in Figure 2a. Note that OMS-2 prepared by the reflux method (Figure 2a) has considerably broader diffraction peaks than that prepared by method 2, implying that the former has smaller particle sizes and larger surface areas than the latter.

To study the effect of counteractions,  $NaMnO_4$ ,  $CsMnO_4$ ,  $Ca(MnO_4)_2$ ,  $Mg(MnO_4)_2$ , and  $Ba(MnO_4)_2$  were used as the source of permanganate. For  $Na^+$ ,  $Mg^{2+}$ , and  $Ca^{2+}$ , X-ray diffraction data show that the products are not cryptomelane, but a poorly crystalline form of nsutite, which is a  $1 \times 2$  intergrowth structure. For  $Ba^{2+}$  and  $Cs^+$ ,

(20) O'Young, C. L. In *Expanded Clays and Other Microporous Solids*; Occelli, M. L., Robson, H., Eds.; Vol. II, 333–340.

(21) Bish, D. L.; Post, J. E. *Am. Miner.* **1989**, *74*, 177.

(22) Faulring, G. M.; Zwicker, W. K.; Forggeng, W. D. *Am. Miner.* **1960**, *45*, 946.

(23) Wakeham, S.; Carpenter, R. *Chem. Geol.* **1974**, *13*, 39.

(24) Brouet, G.; Chen, X. H.; Lee, C. W.; Kevan, L. *J. Am. Chem. Soc.* **1992**, *114*, 3720.

(25) Bystrom, A.; Brystrom, A. M. *Nature*, **1949**, *164*, 1128–1130.

(26) Dargo, R. S. *Physical Methods for Chemists*; Saunders College Publishing: Forth Worth, TX, 1992.

(27) Nam, S. S.; Iton, L. E.; Suib, S. L.; Zhang, Z. *Chem. Mater.* **1989**, *1*, 529.

(28) Post, J. E.; Burnham, C. W. *Am. Miner.* **1986**, *71*, 1178–1185.

**Table 1. Effect of Potassium Concentration on the Synthesis of K-OMS-2**

KMnO <sub>4</sub> /[KMnO <sub>4</sub> ] + [MnSO <sub>4</sub> ]	refluxed	autoclaved <sup>a</sup>
0.88	H <sup>b</sup>	H
0.74	H	H
0.41	H	H
0.36	H	H (major) and N
0.32	H poor	N (major) and H
0.28	H poor	N
0.26	H poor	N

<sup>a</sup> See ref 14. <sup>b</sup> H, hollandite; N, nsutite; H, poor indicates hollandite peaks with poor crystallinity.

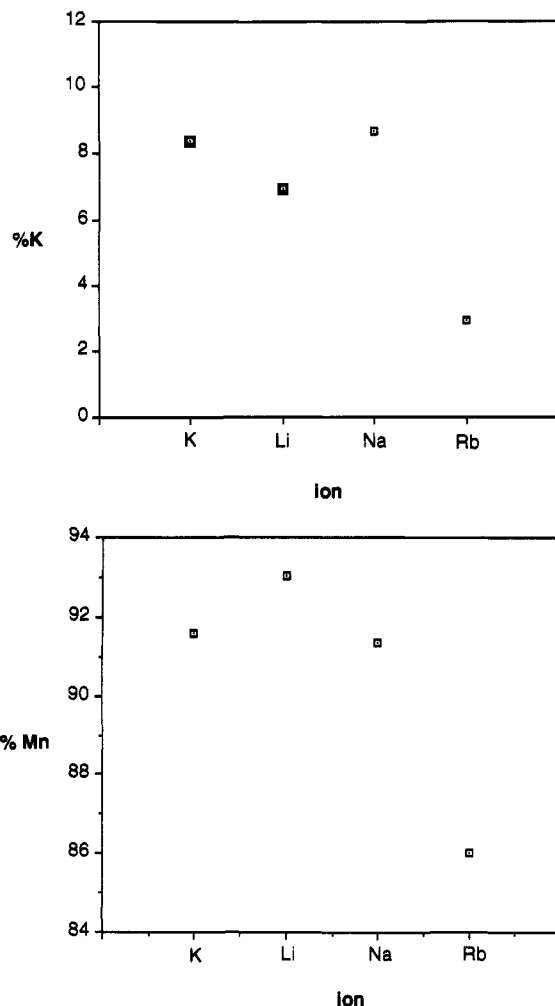


**Figure 3.** Plot of percent K and Mn in ion-exchanged OMS-2 materials stirred with Li<sup>+</sup>, Na<sup>+</sup>, and Rb<sup>+</sup> chlorides.

XRD data show that the products formed have the hollandite structure with either Ba<sup>2+</sup> or Cs<sup>+</sup> as cations. Similar results were observed by O'Young<sup>20</sup> when reaction solutions were autoclaved.

The amount of counteraction in the synthesis of OMS-2 using method 1 is also important. Table 1 shows the effect of changing the amount of K<sup>+</sup> and the product formed using reflux methods. Analytical data are compared for refluxed and autoclaved<sup>20</sup> reaction mixtures heated to similar temperatures. At lower K<sup>+</sup> concentrations, nsutite formed when prepared by autoclave methods, but refluxing, even at low K<sup>+</sup> concentration, produced OMS-2. However, when the concentration of K<sup>+</sup> becomes low, the crystallinity as monitored by XRD becomes poor.

**Chemical and Thermal Analyses.** When OMS-2 prepared by refluxing procedures was ion-exchanged by

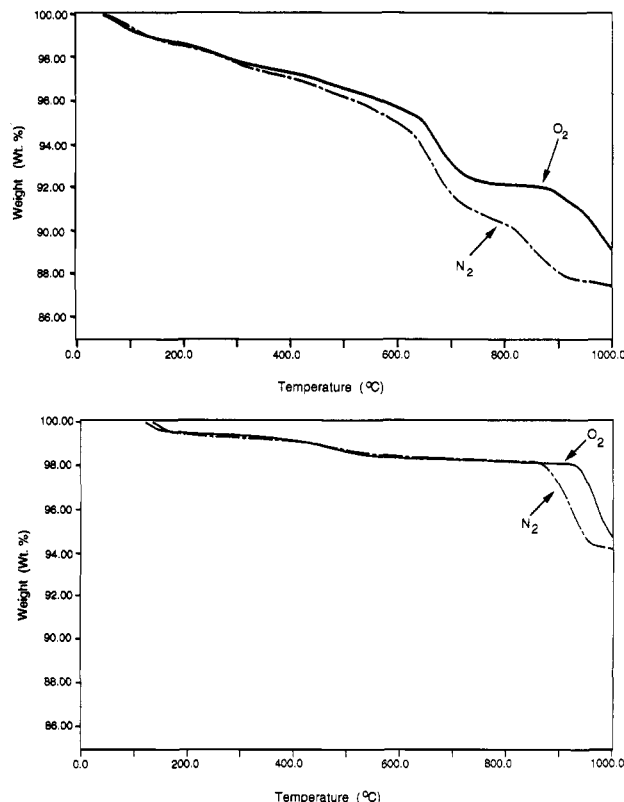


**Figure 4.** TGA of hollandites prepared by (a) refluxing and (b) calcination. The TGA plot recorded with oxygen gas purge is superimposed on the TGA plot obtained by nitrogen gas purge.

**Table 2. Average Oxidation States of Manganese in the Different Cryptomelanes**

method of preparation	% Mn	ave Mn oxidation states
calcined 800 °C	55.6 ± 0.4 <sup>a</sup>	3.68 ± 0.02
refluxed	58.4 ± 0.9	3.80 ± 0.02
autoclaved	56.4 ± 1.2	3.96 ± 0.02

<sup>a</sup> Errors are given as standard deviations.

stirring 0.2 g of cryptomelane in 100 mL of 1 M Li<sup>+</sup>, Na<sup>+</sup>, and Rb<sup>+</sup>, EDX data showed that the percent K in the original OMS-2 decreased markedly for Rb<sup>+</sup>, while remaining fairly the same for the OMS-2 samples stirred in Li<sup>+</sup> or Na<sup>+</sup> as shown in Figure 3. This suggests that Rb<sup>+</sup> can replace some of the K<sup>+</sup>, in this case, about 5% of the K in the OMS-2 tunnel system. Li<sup>+</sup> and Na<sup>+</sup> may be too small to be retained in the tunnel upon washing.

Thermogravimetric analysis (TGA) experiments carried out in nitrogen and oxygen atmospheres of cryptomelanes prepared by refluxing (OMS-2) and by the calcination method are summarized in Figure 4. OMS-2 materials formed using method 1 with autoclaving methods showed identical thermal behavior to cryptomelane formed by refluxing since their TGAs were identical to data presented in Figure 4a. The most striking difference in thermal properties of all these materials is the thermal stability of the calcined cryptomelane. This calcined cryptomelane material is thermally stable up to about 900 °C while the OMS-2 materials prepared by refluxing or autoclaving procedures are stable only to about 600 °C. For the calcined cryptomelane, oxygen evolution, as seen from the difference of the TGA data in nitrogen and oxygen atmospheres, occurs at about 850 °C. The cryptomelane structure is completely reduced to the Mn<sub>3</sub>O<sub>4</sub> spinel structure above 850 °C. For the refluxed and autoclaved OMS-2 materials, oxygen evolution starts at about 400 °C

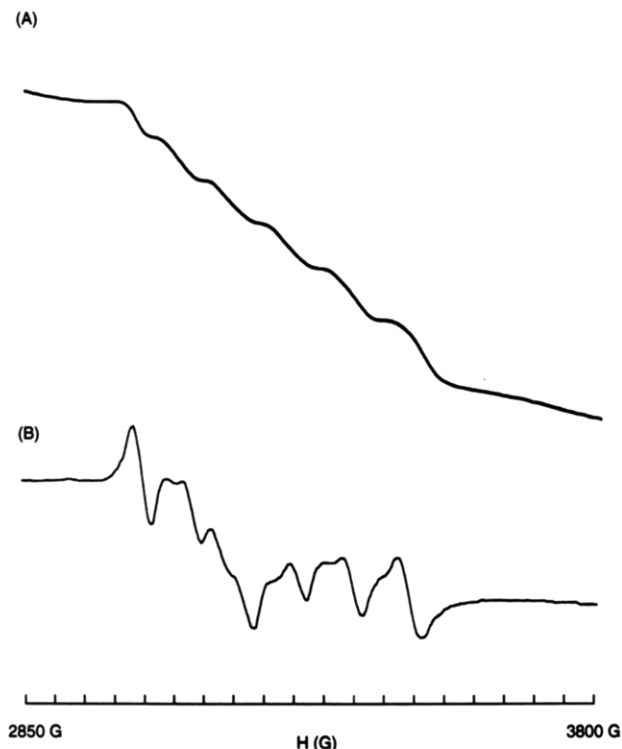


**Figure 5.** X-band EPR spectra at 77K for (a) Fe-OMS-2 and (b) Cu-OMS-2.

and continues up to the maximum temperature (1000 °C) used in the TGA measurement. The refluxed OMS-2 transforms first into  $Mn_2O_3$  at about 600 °C and then at 800 °C transforms into the  $Mn_3O_4$  spinel structure.

**Oxidation States.** The average oxidation states of Mn in the three different synthetic hollandites were determined by iodometric titrations. Table 2 summarizes these results. All the cryptomelane and hollandite samples have average oxidation states from 3.68 to 3.96. The calcined cryptomelane gives the lowest Mn oxidation state, while the autoclaved OMS-2 gives the highest oxidation state. The oxidation number of Mn in OMS-2 is mostly in the 4<sup>+</sup> state, with some in the 3<sup>+</sup> state.

Figure 5a shows the electron paramagnetic resonance (EPR) spectrum of Fe-OMS-2. This Fe-OMS-2 sample was synthesized in the presence of 0.1 M  $Fe^{3+}$  and shows six EPR lines with a  $g$  value of 2.0 and an  $A$  value of 90 G. Fe-OMS-2 synthesized in the presence of 0.01 M  $Fe^{3+}$  showed no such six-line pattern. The attempt to synthesize OMS-2 materials with higher amounts of  $Fe^{3+}$  (0.4 M) was unsuccessful, the result was a black solution after 24 h of refluxing.

When OMS-2 was synthesized using method 1 in the presence of  $Cu^{2+}$ , EPR data showed a six-line pattern. Figure 5b shows the EPR spectrum taken at 77 K of Cu-OMS-2 prepared with a 0.4 M  $Cu^{2+}$  solution. The six lines have a  $g$  value of 2.01 as well as a component due to  $Cu^{2+}$  at a value of  $g$  of 2.02. The hyperfine splitting constant for the six  $Mn^{2+}$  lines is 85 G. OMS-2 materials prepared at lower  $Cu^{2+}$  concentrations (0.1 and 0.01 M) did not show a six-line pattern.

Figure 6 shows the general fibrous morphology of a K-hollandite material. A corresponding electron diffraction pattern for this material is shown in Figure 7. Similar data were observed for various hollandite and cryptomelane materials.



**Figure 6.** Transmission electron micrograph of OMS-2. Magnification is 380 000X.

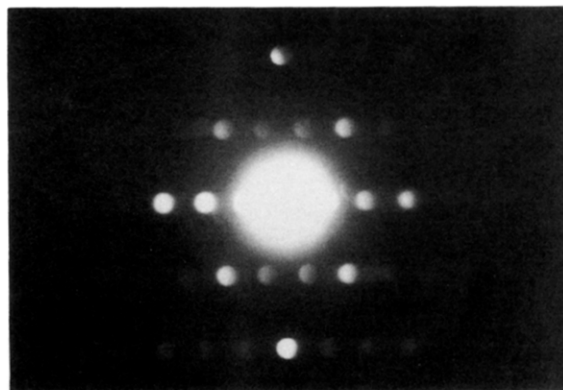


**Figure 7.** Electron diffraction pattern for OMS-2.

## V. Discussion

**Structural and Morphological Studies.** The basic structure of hollandite having  $K^+$  cations in the  $2 \times 2$  tunnel (so-called cryptomelane) depicted in Figure 1 has been prepared by a variety of synthetic procedures described above. The X-ray powder diffraction data of all these systems are similar to the XRD pattern of Figure 2 although differences in cation content do cause changes in relative intensities of peaks. The differences in materials prepared by reflux, calcination, and autoclave procedures described above mainly are primarily manifested (vide infra) in thermal stabilities, average oxidation states for manganese and resultant chemical (i.e., ion exchange) and physical (particle size, surface area) properties.

Data of Figure 2a clearly show that OMS-2 produced by reflux methods have broad lines indicative of smaller particle sizes and larger surface areas than materials produced by autoclave methods. Synchrotron powder

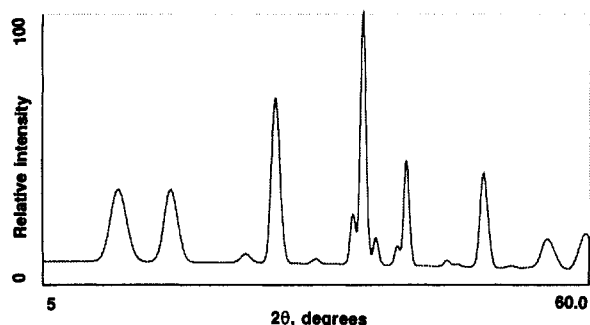


Figure 8. Simulated X-ray diffraction pattern for OMS-2.

Table 3. Rietveld Refinement Parameters for Refluxed K-Hollandite (Cryptomelane, Space Group Tetragonal,  $I4/m$ , Crystallographic Coordinates from Refined Diffraction Pattern)<sup>a</sup>

atom	identity	X	Y	Z	occupancy
K	K <sup>+</sup>	0.00000	0.00000	0.00000	0.60000
Mn1	Mn <sup>4+</sup>	0.85350	0.32955	0.00000	0.80000
Mn2	Mn <sup>3+</sup>	0.85350	0.32955	0.00000	0.20000
O1	O <sup>2-</sup>	0.65529	0.28683	0.00000	1.00000
O2	O <sup>2-</sup>	0.04481	0.36943	0.00000	1.00000

<sup>a</sup>  $a = 9.9172$ .  $c = 2.2738$ . PV-gamma = 0.2.  $R_{wp} = 0.234\ 797$ .

diffraction studies done by spinning the sample confirm that the data of Figure 2a are indeed due to small particle sizes and not due to preferential orientation.<sup>29</sup> The  $2 \times 2$  octahedral  $MnO_6$  units shown in Figure 1 stabilize the general structure of cryptomelane. This structure has been simulated based on the  $I4/m$  tetragonal space group and has been used to simulate the XRD pattern of Figure 8 for K-OMS-2.

Comparison of the data of Figure 8 to the experimental data of Figure 2 shows a good match of the positions of the diffraction lines. The relative intensities of the simulated XRD pattern of Figure 8 do not exactly match the experimental data of Figure 2. This may be due to an incomplete detailed analysis of the location of all K<sup>+</sup> ions, due to defects in the lattice (primarily O defects), the small crystal size and poor crystallinity of the K-OMS-2 materials, lattice imperfections, preferential ordering or other factors.

A fibrous morphology as shown in Figure 6 is typical for hollandite materials. The TEM data of Figures 6 and 7 show that the K<sup>+</sup> hollandite (OMS-2) fibers are single crystals and are of different morphology and structure than OMS-1 materials having a todorokite structure (see Figure 1) reported previously.<sup>1,2</sup> The electron diffraction data for K-hollandite shown in Figure 7 have also been simulated and there is an excellent match suggesting that K<sup>+</sup> ions are primarily located in the tunnels of OMS-2 (cryptomelane) and that these are single phase materials. These TEM data are also in good agreement with X-ray data (Figures 2 and 8).

Results of the Rietveld refinement of the more poorly crystalline refluxed cryptomelane are summarized in Table 3. The tunnel cation position was not included in the refinement.<sup>18</sup> Table 1 provides a summary of the parameters refined during the procedure. The refined  $a$  lattice parameter is 9.9172 and the  $c$  lattice parameter is 2.2738. The final  $R_{wp}$  is 0.235. The assumption of tetragonal  $I4/m$  symmetry appears to be justified. The tunnel cation positions appear to be disordered. These refinement data

suggest that the structure of OMS-2 is similar to phases produced by flux methods,<sup>17</sup> however there is a considerable lengthening of  $a$  (from 9.87 Å) and shortening of  $c$  (from 2.87 Å) as well as major differences in particle size.

**Stability of Hollandites.** Thermogravimetric analyses (TGA) of hollandite samples prepared by refluxing, autoclaving, and calcination showed differences in their thermal behavior. OMS-2 materials formed by refluxing and autoclaving showed identical TGA data for experiments with either nitrogen or oxygen atmospheres. Together with the X-ray diffraction data, the two methods seem to form the same types of OMS-2 material. This is an indication that the use of autogenous pressure has no effect on the synthesis of OMS-2 by method 1.

Figure 4a shows the TGA under nitrogen and oxygen atmospheres of OMS-2 formed by refluxing. When TGA was done under oxygen atmosphere, there is a gradual weight loss from room temperature to 650 °C, where a phase transition occurs from cryptomelane to  $Mn_2O_3$  as detected by XRD. The  $Mn_2O_3$  phase remains stable up to about 900 °C where transformation to  $Mn_3O_4$  occurs as observed by XRD. From the TGA done under nitrogen atmosphere, oxygen evolution starts at about 300 °C and continues throughout the temperature range used in the TGA experiment. Oxygen stabilizes the  $Mn_2O_3$  phase formed and retards the transition temperature of  $Mn_2O_3$  to  $Mn_3O_4$  by almost 70 °C. The transition from cryptomelane to  $Mn_2O_3$ , however, occurs at even higher temperature (385 °C) under oxygen atmosphere. Oxygen evolution is greater for the transformation of  $Mn_2O_3$  to  $Mn_3O_4$  than for the hollandite to  $Mn_2O_3$  transition.

Previous work on the thermal properties of naturally occurring hollandite, cryptomelane, and coronadite showed that heating these minerals resulted in the evolution of water and oxygen with subsequent Mn reduction.<sup>21</sup> The stepwise transformations of cryptomelane to bixbyite and hausmannite were monitored by X-ray diffraction.<sup>22</sup>

Cryptomelanes formed by method 2 contain less water due to the high temperature used in the synthesis. This is seen from the slope of the TGA curve for calcined hollandite (Figure 4b) where the weight loss is practically level up to 130 °C. There is a weight loss at 130–150 °C, and a gradual weight loss from 150 to 350 °C. From 350 to 550 °C, there is a significant weight loss, whereupon the weight stabilizes up to about 950 °C in an oxygen atmosphere or 860 °C in a nitrogen atmosphere. X-ray diffraction data revealed no different manganese oxide phases, until the temperature reaches about 900 °C where  $Mn_3O_4$  forms. The difference in the transition temperature when TGA is done in oxygen and nitrogen atmospheres indicates oxygen evolution accompanying the transformation. Figure 4b indicates that there is a significant oxygen evolution during the transformation of cryptomelane to  $Mn_3O_4$  at about 860 °C.

Hollandites formed by different methods have different thermal properties. Oxygen evolution occurs at lower temperature, at about 300 °C for OMS-2 formed by refluxing, than for hollandite formed by calcination. In the latter, oxygen evolution occurs at higher temperature, at about 900 °C. The amount of oxygen evolved, based on the difference between the TGA plots under nitrogen and oxygen atmospheres, is much more for refluxed OMS-2 than for calcined hollandite. The amount of oxygen evolved for refluxed OMS-2 is about 77% larger than that for calcined hollandite.

(29) Hriljac, J.; Suib, S. L. 1994, unpublished results.



Ion-exchange data for OMS-2 shown in Figure 3 as well as data of Table 1 suggest that the  $[K^+]$  is an important factor for growth and stability of OMS-2. The ion-exchange data of Figure 3 clearly indicate that  $Rb^+$  prefers the tunnel sites of OMS-2 with respect to other alkali metals at least during ion-exchange.

**Oxidation States of Elements of Hollandite.** Thermal studies of calcined cryptomelane suggest that water and oxygen are removed from the cryptomelane structure. Calcination also decreases the oxidation state of manganese. This is seen in Table 2 which shows the average oxidation state of the calcined, refluxed, and autoclaved cryptomelanes. The primary manganese oxidation states in hollandite are 4+ and 3+. The lower values of Table 2 indicate the presence of more  $Mn^{3+}$ . From this, the amount of  $Mn^{3+}$  increases from autoclaved to refluxed and to calcined cryptomelane.

Naturally occurring hollandite and cryptomelane have been shown to contain manganese in the 4+ and 3+ states by spectroscopic methods or as determined by single-crystal X-ray diffraction.<sup>5</sup> Todorokite [OMS-1], a related manganese oxide with the  $3 \times 3$  structure, is believed to contain  $Mn^{2+}$  from X-ray diffraction studies.<sup>5</sup> This has been confirmed by EPR studies of synthetic todorokite<sup>1-3</sup> which showed well-resolved  $Mn^{2+}$  lines. Another EPR study<sup>23</sup> on manganese nodules identified tetrahedral  $Fe^{3+}$  and  $Mn^{2+}$  but no indication of  $Co^{2+}$ ,  $Ni^{2+}$ , and  $Cu^{2+}$ . A significant result of the present study is the identification of  $Mn^{2+}$  by EPR methods when OMS-2 was synthesized in the presence of  $Cu^{2+}$  and  $Fe^{3+}$ . X-ray diffraction data for OMS-2 materials synthesized in the presence of other transition-metal ions such as  $Ni^{2+}$ ,  $Co^{2+}$ , and  $Cr^{3+}$  showed the formation of the hollandite structure, but EPR did not indicate the presence of  $Mn^{2+}$ . It is possible that incorporation of  $Cu^{2+}$  or  $Fe^{3+}$  in OMS-2 diminishes saturation of  $Mn^{2+}$  that may be present in higher concentration or different sites of other OMS-2 materials that are EPR silent. In any event it is clear that  $Mn^{2+}$  is present in these materials. This may explain the ability of OMS-2 to incorporate other divalent cations like  $Cu^{2+}$ ,  $Co^{2+}$ , or  $Ni^{2+}$  via either ion-exchange (Figure 3) or isomorphous substitution.<sup>1-4</sup>

Hollandites, together with other types of manganese oxide minerals, such as todorokites and birnessites, are found in deep sea manganese nodules and may provide an economic resource for copper and nickel. OMS-2 materials were synthesized in the presence of other transition metal ions like  $Cu^{2+}$  or  $Fe^{3+}$  to study if such ions can be incorporated in synthetic manganese oxide systems. The most significant result as regards synthetic strategies for making OMS materials is the detection of non-exchangeable octahedral  $Mn^{2+}$  in the OMS-2 structure as identified by electron paramagnetic resonance (EPR). These data suggest that OMS-2 materials have a similar range of oxidation states for manganese ( $Mn^{2+}$ ,  $Mn^{3+}$ ,  $Mn^{4+}$ ) as for OMS-1 in contrast to natural materials ( $Mn^{3+}$ ,  $Mn^{4+}$ ).<sup>5-16</sup> This may allow preparation of novel OMS systems with unique electronic and catalytic applications.

The EPR spectrum of Fe-OMS-2 (Figure 5a) seems to be a superposition of two lines with almost similar  $g$  values, one broad line, and one with six hyperfine lines. The six lines are due to isolated  $Mn^{2+}$  ions, and the  $g$  value of 2.0 and an  $A$  value of 90 gauss suggest that the environment of  $Mn^{2+}$  is octahedral.<sup>26</sup>  $Mn^{2+}$  in a tetrahedral environment will have an  $A$  value of about 80 G or lower. The broad

line at a  $g$  value 2.0 could be due to  $Mn^{2+}$  in different sites, or it could be due to  $Fe^{3+}$  in octahedral sites. Octahedral  $Fe^{3+}$  has a  $g$  value of 2.0, while tetrahedral  $Fe^{3+}$  has a  $g$  value of about 4.2.<sup>27</sup> Kevan and co-workers<sup>24</sup> studying the EPR of  $Mn^{2+}$  in molecular sieves have observed overlapping of  $Mn^{2+}$  EPR lines, one broad, and one with resolved six lines when  $Mn^{2+}$  ions are in two different environments. The broadening of the  $Mn^{2+}$  line could also be due to spin-spin interactions.

The Cu-OMS-2 system contains two EPR lines (Figure 5b), one six-line pattern which is due to  $Mn^{2+}$  hyperfine with a  $g$  value of 2.01 and an  $A$  value of 85 G. The other EPR signal with a  $g$  value of 2.02 is due to  $Cu^{2+}$  in an axial environment and is the perpendicular component. The parallel component of the  $Cu^{2+}$  hyperfine is not observed.<sup>26</sup> The superposition of the manganese and copper lines may make the parallel component of the  $Cu^{2+}$  hyperfine difficult to observe. It is highly probable, based on the  $g$  value of the perpendicular component, that  $Cu^{2+}$  is in a distorted octahedral environment in the OMS-2 structure.<sup>26</sup> This result may also support the observation of less crystalline (Figure 2a) OMS-2 materials that are strained by incorporation of divalent cations.

## Conclusions

Hollandites prepared by different methods showed different thermal properties. Powder X-ray diffraction data showed that the structures of hollandites formed via different routes are very similar although particle sizes and surface areas can be different. The average oxidation states of the manganese present in the synthetic hollandites showed differences also, based on the method of preparation which suggests that a range of materials with variable compositions can be prepared. Hollandite formed by calcination at higher temperatures showed smaller Mn average oxidation state than OMS-2 materials formed by refluxing or autoclaving. This indicates that the Mn in the calcined hollandite has more manganese in the  $Mn^{3+}$  state. This is important since the lower the average manganese oxidation state, the higher the cation exchange capacity and ability to produce materials with a wider composition. The most prevalent Mn oxidation states for these hollandites are the  $Mn^{4+}$  and  $Mn^{3+}$  states. However, when OMS-2 was prepared by refluxing in the presence of  $Cu^{2+}$  or  $Fe^{3+}$  ions, EPR data clearly show that  $Mn^{2+}$  is present. Powder X-ray diffraction confirmed the hollandite structures of these Cu- or Fe-OMS-2 materials indicating relatively pure phases. Electron and X-ray diffraction simulations are found to agree well with experimental data for hollandite OMS-2 type structures. All of these results suggest that the compositional and electronic properties of OMS-2 can be tailored. Resultant electrochemical,<sup>3</sup> catalytic,<sup>12</sup> magnetic,<sup>4</sup> and conductivity<sup>3</sup> properties are clearly dependent on balancing these manganese valence states as well as the resulting chemical compositions.

**Acknowledgment.** We acknowledge Texaco, Inc., and the Department of Energy, Office of Basic Energy Sciences, Division of Chemical Sciences for support of this research. We thank L. McCurdy and D. I. Potter for collecting the TEM data.